Structures of metal nanoparticles adsorbed on MgO(001). II. Pt and Pd

ARTICLE *in* THE JOURNAL OF CHEMICAL PHYSICS · MAY 2009

Impact Factor: 2.95 · DOI: 10.1063/1.3121307 · Source: PubMed

10 AUTHORS, INCLUDING:

Giovanni Barcaro
Italian National Research Council
106 PUBLICATIONS **1,598** CITATIONS
SEE PROFILE

Alessandro Fortunelli
Italian National Research Council
210 PUBLICATIONS **3,986** CITATIONS
SEE PROFILE

Giulia Rossi
Università degli Studi di Genova
55 PUBLICATIONS **1,630** CITATIONS
SEE PROFILE

Riccardo Ferrando
Università degli Studi di Genova
234 PUBLICATIONS **8,376** CITATIONS
SEE PROFILE

Structures of metal nanoparticles adsorbed on MgO(001). II. Pt and Pd

Jacek Goniakowski,[1,a)] Andrei Jelea,[2,3] Christine Mottet,[2] Giovanni Barcaro,[4] Alessandro Fortunelli,[4] Zdenka Kuntová,[5,6] Florin Nita,[5,3] Andrea C. Levi,[5] Giulia Rossi,[5] and Riccardo Ferrando[5,a)]

[1]*INSP/CNRS and Université Paris VI, Campus Boucicaut, Paris, 75015, France*
[2]*CINaM/CNRS, Campus de Luminy, Marseille, 13288, France*
[3]*Institute of Physical Chemistry Ilie Murgulescu, Romanian Academy, 202 Spl Independentei St., 060021 Bucharest-12, Romania*
[4]*IPCF/CNR, via G. Moruzzi 1, Pisa, 56124, Italy*
[5]*Dipartimento di Fisica, CNISM and INFM/CNR, Via Dodecaneso 33, Genova, 16146, Italy*
[6]*Institute of Physics, AS CR, v.v.i., Na Slovance 2, 182 21 Prague 8, Czech Republic*

(Received 4 November 2008; accepted 30 March 2009; published online 1 May 2009)

The structure of metal clusters on MgO(001) is searched for by different computational methods. For sizes $N \leq 200$, a global optimization basin-hopping algorithm is employed, whereas for larger sizes the most significant structural motifs are compared at magic sizes. This paper is focused on Pt and Pd/MgO(001), which present a non-negligible mismatch between the nearest-neighbor distance in the metal and the oxygen-oxygen distance in the substrate. For both metals, a transition from the cube-on-cube (001) epitaxy to the (111) epitaxy is found. The results of our simulations are compared to experimental data, to results found for Au and Ag in the previous paper (paper I), and to predictions derived from the Wulff–Kaischew construction. © *2009 American Institute of Physics*. [DOI: 10.1063/1.3121307]

I. INTRODUCTION

In the previous paper (I),[1] we searched for the lowest-energy structures of Au and Ag nanoparticles supported on MgO(001) by global optimization methods and by comparing the most significant structural motifs at large sizes. Since the nearest-neighbor distance in bulk Au and Ag is of 2.88 and 2.89 Å, respectively, these metals present a rather small lattice mismatch with the oxygen-oxygen distance in the substrate, about 3%. In this paper (II) we focus on Pt and Pd, whose bulk lattice spacings are smaller so that their lattice mismatch with the substrate is more important, being 7.0% and 7.6%, respectively. A larger lattice mismatch can have strong effects on the preferred epitaxy on the substrate. For example, in the cases of Ni/MgO(001), Pd/CaO(001), and Pt/CaO(001), which present an even larger mismatch, the interaction with the substrate stabilizes hcp phases.[2,3] For Pd and Pt/MgO(001) we do not expect this behavior.[2] Nevertheless, we expect that lattice mismatch can play a role in determining structural transitions between fcc epitaxies. In addition, Pd and Pt differ from Ag and Au also because they present a stronger interaction with the substrate.

The computational methodology is described in paper I. Here, in Secs. II and III we discuss the global optimization results and the comparison of structural motifs for Pt and Pd, respectively. In Sec. IV, the results are rationalized in terms of the Wulff–Kaischew construction,[4,5] modified in order to take into account the variation in adhesion energy with the size of the clusters.[6] Section V contains an overall discussion of all the systems treated in papers I and II.

II. PT NANOPARTICLES

A. Global optimization results

In the size range up to 200 atoms, we considered the following sizes: $N=30,40,50,60,70,90,100,150,200$, finding that fcc(001) structures are always the lowest in energy, followed by decahedral and fcc(111) clusters. The only exception is $N=200$, at which the fcc(111) motif is slightly lower in energy than decahedra. Icosahedral particles are higher in energy. Only for $N=50$ we find an icosahedron whose energy is close (but still higher) than the best fcc(111) cluster. These results show once more the importance of the substrate in determining the most stable cluster structures. In fact, within the same model potential, free Pt clusters would be preferentially decahedral in this size range.[7,8]

In Fig. 1 we report an example of this behavior, for size $N=90$. At this size, the global minimum [Fig. 1(a)] is an fcc(001) cluster, which presents stacking faults (one of them gives a twin boundary). Clusters of this kind are often the global minima, at variance with the results for Au and Ag.[1] However, we note that our model for the Pt–Pt interaction underestimates the stacking fault energy, so that the appearance of such faults might be facilitated by this feature. In any case, fcc(001) clusters without faults are also found [Fig. 1(b)] and they are lower in energy than decahedra and fcc(111) structures [Figs. 1(c) and 1(d), respectively]. Especially the latter are much higher in energy, not only for $N=90$ but in the whole size range up to 200 atoms.

[a)]Authors to whom correspondence should be addressed. Electronic addresses: jacek.goniakowski@insp.jussieu.fr and ferrando@fisica.unige.it.

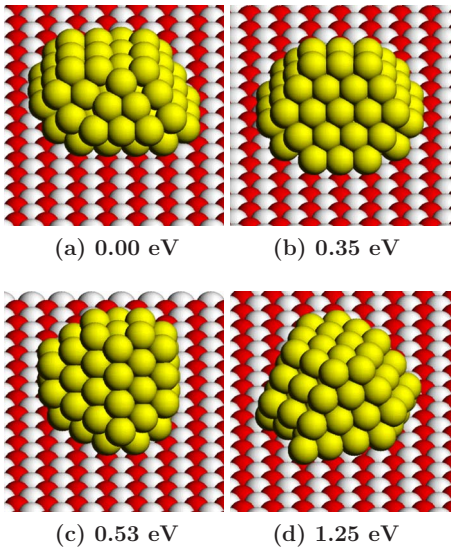

FIG. 1. (Color online) Pt/MgO(001) nanoparticles of size $N=90$.

B. Comparison of selected structural motifs for large sizes

The comparison of fcc(001), fcc(111), and decahedral structures (see Fig. 2) confirms that, for $N<200$, fcc(001) clusters are the lowest in energy, followed by decahedra and fcc(111) clusters. A first crossover between fcc(111) and decahedral clusters takes place around size 200, while the crossover between fcc(001) and fcc(111) structures is around $N=550$. From this size on, the fcc(111) structures are the most stable. This estimate, deduced from results on the magic clusters only, is necessarily approximative. Indeed, a detailed set of results (inset of Fig. 2) shows very similar energies of the two motifs in a relatively large zone of cluster sizes, where an addition or subtraction of a single atom may change their relative stability, as checked also by global optimization runs in the vicinity of size 400. Even though the crossover zone is broadened in a size range of more than 100

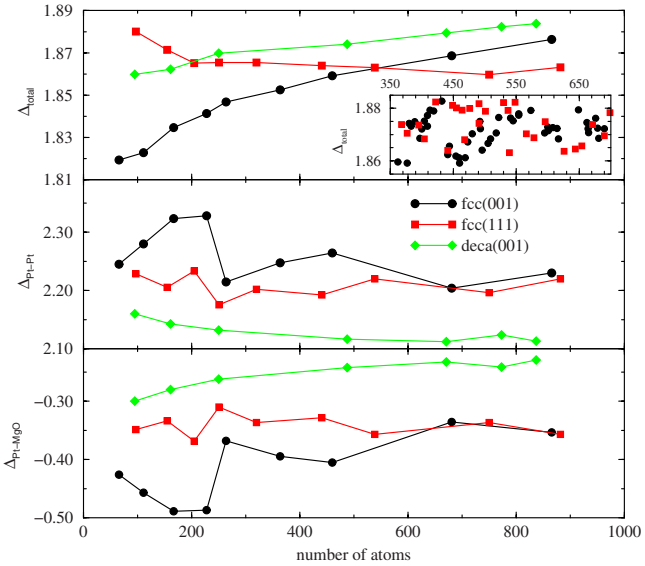

FIG. 2. (Color online) Δ_{total}, Δ_{Pt-Pt}, and Δ_{Pt-MgO} (in eV) for fcc(001), fcc(111); and decahedral Pt nanoparticles. A detailed representation of the fcc(001)→fcc(111) transition zone is given in the inset.

atoms, the crossover is however much sharper than in gold,[1] where epitaxies compete in a range of width of about 10^3 atoms at least.

Decomposing the energy into a metal-metal part and a metal-oxide part, we find that decahedral structures present the lowest metallic energy (as expected for free clusters[7,8]) and the weakest interaction with the substrate. On the other hand fcc(111) clusters are better than fcc(001) clusters for what concerns the metallic energy and worse for what concerns the interaction with the substrate.

This is a general behavior, which is similar to the Ag and Au cases as described in paper I.[1] However, in Pt, the adhesion of fcc(111) clusters becomes almost as good as the adhesion of fcc(001) clusters as size increases. In fact, at variance with Ag and Au, the adhesion energy of the (001) epitaxy does not evolve in a monotonic way: Around 250 atoms in size, the adhesion energy decreases abruptly in absolute value because of a partial relaxation of the epitaxial strain due to the variation in size of the surface in contact with the support (the full strain release by interfacial dislocations[9,10] takes place at larger size than those displayed in Fig. 2). This partial relaxation is sufficient to make (001) adhesion energy of the same magnitude as the (111) adhesion energy. This behavior also appears in Pd (as we will show in the following) and leads to a structural crossover.

Platinum films have been grown on the MgO(001) surface by a variety of techniques, including pulsed laser deposition,[11–14] electron beam evaporation,[15–17] and sputtering.[18–21]

As a general trend, it has been found that the (111) and (001) epitaxies coexist at low temperature and the (001) one tends to dominate in films obtained at higher temperatures. For example, *in situ* analysis by grazing incident small angle x-ray scattering (GISAXS) of Pt grown by physical evaporation shows that for growth at 1000 K and even after annealing at 1500–1600 K, the cluster epitaxy is the (001) whereas the clusters grown below 1000 K display preferentially the (111) epitaxy.[22] Nanoparticle structural transformations depending on coverage (which determines the cluster size) or temperature have been observed also in other systems, such as In/Si(111) growth[23] or Ni/MgO(001).[2] For In/Si(111), it was possible to determine experimentally the kinetic pathways for the fcc(111)→bct(101) transformation obtained by either increasing the thickness of the deposited In film or the temperature. In the case of Pt/MgO(001) experimental information on a possible epitaxy change depending on cluster size is not yet available and therefore a direct quantitative comparison with our simulations is not yet possible.

However, our results are in qualitative agreement with the experimental findings in predicting that both epitaxies should be observed as low-temperature structures, provided that the structures observed below 1000 K are close to those expected at equilibrium. In any case, it is difficult to rule out possible kinetic or thermodynamic effects[8] in order to establish whether the experimentally produced clusters really represent the low-temperature equilibrium structures.

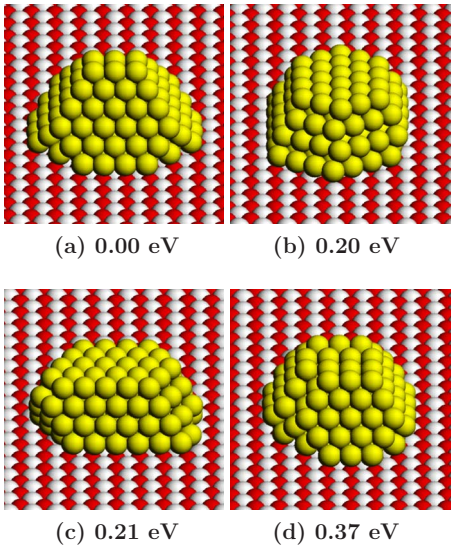

FIG. 3. (Color online) Pd/MgO(001) nanoparticles of size $N=150$.

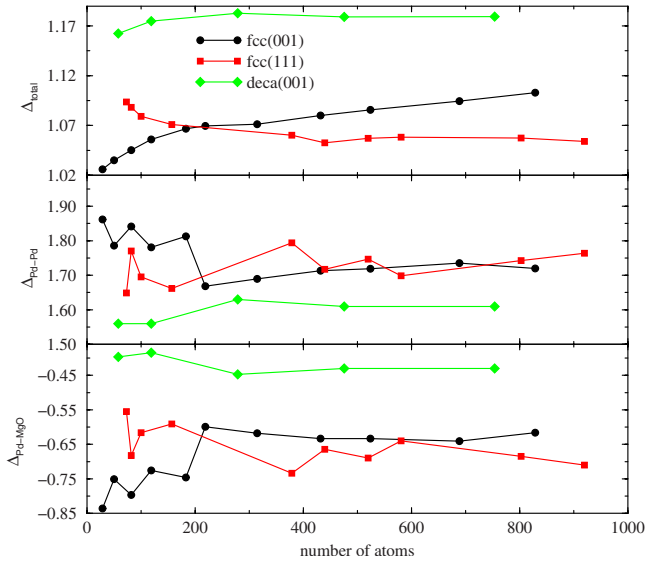

FIG. 4. (Color online) Δ_{total}, Δ_{Pd-Pd}, and Δ_{Pd-MgO} (in eV) for fcc(001), fcc(111), and decahedral Pd nanoparticles.

In fact, kinetic trapping effects are very difficult to avoid in low-temperature experiments. Growing clusters tend to get trapped into metastable structures that belong to the same motif, which is produced at lower sizes. A clear example has been found in the growth of gas-phase silver clusters simulated by molecular dynamics.[24] There, icosahedral clusters are produced for large sizes, at which icosahedra are much higher in energy than decahedra or fcc clusters. These metastable structures can have quite long lifetimes. Even though the growth on surfaces takes place on longer time scales than aggregation in gas phase, we expect for example that the (111) clusters predicted by our model for sizes of about 400 atoms would be very difficult to observe, since smaller clusters (and also some larger clusters) are in (001) epitaxy.

Finally, we note that, since average surface energies calculated for clusters in (001) and (111) epitaxy differ by a few hundredths of J/m^2 only, one cannot exclude that our energetic model is not precise enough. Such a small inaccuracy may indeed be related to the anisotropy factor $\gamma_{(001)}/\gamma_{(111)}$ being underestimated by the present Pt–Pt potential. This factor may play a role in determining the transition size between epitaxies, as will be discussed in Secs. IV and V.

III. PD NANOPARTICLES

A. Global optimization results

The structures of Pd/MgO nanoparticles of sizes $N \leq 120$ have been searched for in Ref. 25 within the same model considered here. In that size range, a clear prevalence of fcc(001) truncated pyramids has been found. These results have been confirmed also by density-functional (DF) theory calculations for $N \leq 34$.[26] In the following we focus on sizes $N > 120$.

For $N=150$, the global minimum is a fcc(001) structure, shown in Fig. 3(a). However, the structures in Figs. 3(b) and 3(c) present close-packed planes in contact with the substrate and are separated from the global minimum by only 0.2 eV. Structure (b) is indeed a hcp cluster with four close-packed planes in *ABAB* stacking. This cluster is obtained by truncating a hexagonal pyramid.[2] The occurrence of hcp clusters in our model might be overemphasized by the fact that our metal-metal interaction produces a small energy difference between fcc and hcp bulk phases. However, structure (c), which is almost degenerate with (b), is a fcc(111) cluster, which is thus in rather close competition with the global minimum. Structure (d) is fcc(001) with an island in stacking fault.

B. Comparison of selected structural motifs for large sizes

From a comparison among structural motifs, a crossover from fcc(001) to fcc(111) structures is predicted for sizes around 200 atoms, as shown in Fig. 4. Decahedral structures are always the highest in energy. The decomposition into metal-metal and metal-substrate contributions shows that, as in the other metals, decahedra present the most favorable metal-metal interaction, which however is overcompensated by a weak adhesion to the substrate.

For small sizes, metallic energy is compensated by the adhesion energy to favor the (001) epitaxy as in the other metals. For $N > 200$, fcc(001) metallic energy falls abruptly, symmetrically compensating the strengthening of the adhesion to the substrate. This corresponds to a partial strain release as in the Pt/MgO case due to the large lattice mismatch. As a result, metallic energies are comparable for both fcc epitaxies, but fcc(111) clusters better adhere to the substrate, which is a particularity of the Pd case because it has never been observed for the other metals. In fact, at best, Pt adhesion energy becomes equivalent for the two fcc epitaxies. This result will be rationalized in Sec. IV in terms of size-dependent adhesion energies per unit area.

The experimental results on Pd/MgO(001) report the observation of mostly fcc(001) nanoparticles,[27] with some evidence in favor of the formation of fcc(111) epitaxy clusters as cluster size increases. This evidence has been reported in recent experiments,[28] in which fcc(111) clusters are observed

TABLE I. Values of σ, τ_1, and τ_2 for the four metals.

Metal	σ	τ_1	τ_2
Ag	0.88	0.58	0.50
Au	0.86	0.71	0.69
Pt	0.85	0.59	0.64
Pd	0.87	1.11	1.21

even for the smallest sizes (4–5 nm). However, these (111) clusters are much larger than our transition size (a few thousand atoms at least compared to 200 atoms). The possible origin of this disagreement will be discussed in Sec. V.

IV. WULFF–KAISCHEW CONSTRUCTION FOR FCC(001) AND FCC(111) EPITAXIES

The shapes and energies of supported clusters can easily be computed in the limit of large clusters by means of the Wulff–Kaischew construction.[4,5] Here we apply this construction not only to Pd and Pt, but also to the metals treated in paper I (Ag and Au). In such limit no reference to the atomic structure is necessary and the shape and energy of a cluster depends on few parameters, i.e., on the surface energies per unit area γ and on the adhesion energy ε, again per unit area, to the substrate. ε is negative being an energy gain. Moreover, it is easy to convince oneself that for the noble and quasinoble metals only facets in the (001) and (111) orientations occur at equilibrium, all other orientations leading to considerably higher surface energies. Within this approach, contributions due to edges and vertices are neglected. Energy contributions due to dislocations are not considered either. Therefore, we expect the Wulff–Kaischew approach to be valid in the limit of large clusters. We do not consider noncrystalline structures because they are not expected to be favorable at large sizes due to their internal strain.

Under these conditions, as shown in detail in the Appendix, all relevant cluster properties, in particular, the equilibrium shape and energy of a cluster, depend on the three ratios

$$\sigma = \frac{\gamma_{(111)}}{\gamma_{(001)}}, \quad \tau_1 = \frac{|\varepsilon_{(001)}|}{\gamma_{(001)}}, \quad \tau_2 = \frac{|\varepsilon_{(111)}|}{\gamma_{(111)}}. \tag{1}$$

A relevant question is whether the cluster prefers to lie on a (001) facet (orientation 1) or on a (111) facet (orientation 2). An answer to this question can be obtained by calculating the energies $E_1(\sigma,\tau_1,\tau_2)$ and $E_2(\sigma,\tau_1,\tau_2)$ of clusters with the same volume but with (001) and (111) epitaxies, respectively. The formulas for E_1 and E_2 are rather cumbersome and are given in the Appendix, along with their derivation.

In the cases studied in the present work (noble and near-noble metal clusters adsorbed on magnesium oxide) the effect of σ is relatively unimportant, because for all considered metals our model predicts that σ values lie in a narrow range $0.85 \leq \sigma \leq 0.88$, while there is much more spread in τ_1 and τ_2, as can be seen in Table I. A convenient way of presenting the results is to consider the (τ_1,τ_2) plane at fixed σ (see Fig. 5).

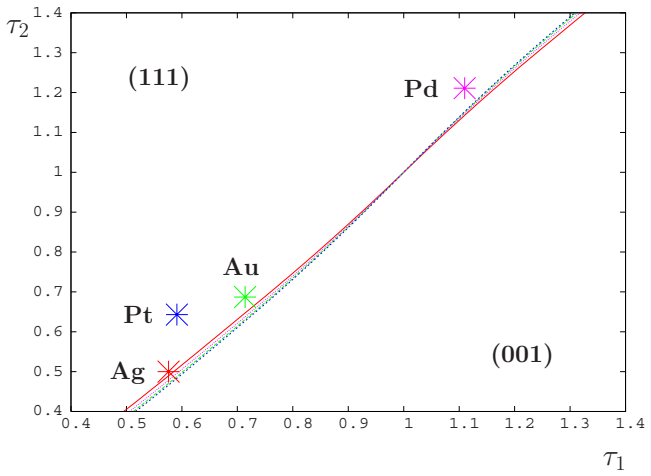

FIG. 5. (Color online) (τ_1,τ_2) plane at fixed σ. The lines separate the upper left part of the plane [where (111) epitaxy is favored] and the lower right part [where (001) epitaxy is favored] for the different metals. The points correspond to the actual values of (τ_1,τ_2) reported in Table I.

This plane is subdivided into two regions, separated by a line which runs near the diagonal $\tau_1=\tau_2$. This line is obtained by imposing that the energies of the two epitaxies are equal, $E_1=E_2$, for the same cluster volume. The line is slightly different for the different metals, corresponding to the small differences in σ. In the upper left region (high τ_2) of the plane, (111) epitaxy is favored, while in the lower right region (high τ_1) (001) epitaxy prevails.

From this plot it turns out that the condition for having the (001) epitaxy preferred over the (111) epitaxy is not simply $\varepsilon_{(001)} > \varepsilon_{(111)}$, but $\tau_1 > \tau_2$. As we shall see below, a larger ε does not translate automatically into a larger τ, because, in metal-oxide systems, a large ε is correlated with a large γ.

The (τ_1,τ_2) values of Table I fall in the region in which (111) epitaxy is favorable for all metals. This means that, asymptotically in the limit of large clusters, all four metals should present a crossover to (111) epitaxy. Note however that the point corresponding to Ag is very close to the separation line, indicating that the stability of the (111) epitaxy should be marginal. These results are in agreement with our simulations, which show a clear crossover toward the (111) epitaxy for Au, Pt, and Pd, while in the case of Ag, the crossover, if any, should be for $N > 3000$.[1]

The Wulff–Kaischew construction simply gives the prevailing structure in the limit of large sizes. In the following we show that this construction can be extended by incorporating size-dependent interface energies[6] to predict the size dependence of the epitaxy. In particular, we demonstrate that, by introducing size-dependent adhesion energies, we are able to reproduce the transition between epitaxies in the correct size range.

First of all, we note that the observed transitions are at rather large sizes, and therefore the contribution of edges and vertices should not be very important, so that the functional form of $E_1(\sigma,\tau_1,\tau_2)$ and $E_2(\sigma,\tau_1,\tau_2)$ can be taken as in the large-size limit discussed before. The size dependence can be introduced in first approximation by letting the parameters σ, τ_1, and τ_2 depend on size, so that also γ and ε depend on size.

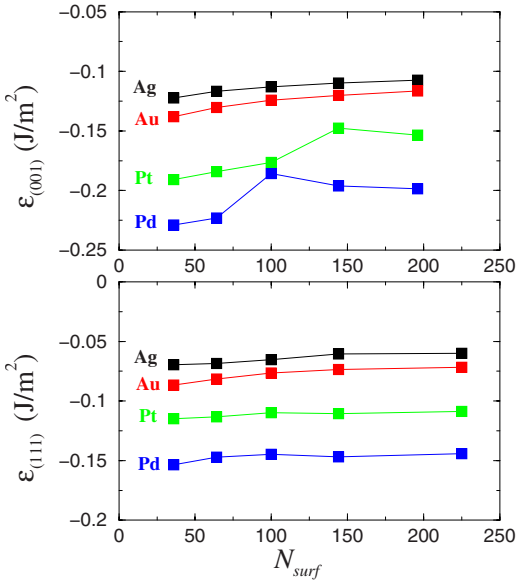

FIG. 6. (Color online) Variation in $\varepsilon_{(001)}$ and $\varepsilon_{(111)}$ with N_{surf} (the number of atom in contact with the substrate) for all metals. Energies are given in J/m^2.

Size-dependent adhesion energies have been calculated considering truncated octahedral clusters at different geometric magic sizes and with aspect ratios corresponding to the lowest energy in each size range. The adhesion energies $\varepsilon_{(001)}$ and $\varepsilon_{(111)}$ significantly depend on size, as shown in Fig. 6, while surface energies γ present a weaker change, at least until clusters become very small. Therefore τ_1 and τ_2 vary with size, with σ remaining constant. In Fig. 6 we report $\varepsilon_{(001)}$ and $\varepsilon_{(111)}$ as a function of the number of cluster atoms in contact with the substrate, N_{surf}. It turns out that decreasing N_{surf} the adhesion energies tend to increase in absolute value, indicating a stronger adhesion per unit area. This is due to an easier accommodation of strain when the number of contact atoms decreases.

For $\varepsilon_{(111)}$ the change with N_{surf} is rather small. For $\varepsilon_{(001)}$ this change is larger, especially in the cases of Pd and Pt, which present a non-negligible lattice mismatch with the substrate. In these cases, the change in the slope around $N_{surf}=100$ corresponds to the introduction of interfacial dislocations.[9,10]

If these variations in $\varepsilon_{(111)}$ and $\varepsilon_{(001)}$ are taken into account a size-dependent crossover from fcc(111) epitaxy at large sizes to fcc(001) epitaxy at small sizes is predicted for all metals, as can be seen in Fig. 7. In this figure, the starting points, which are in the fcc(001) region of the (τ_1,τ_2) plane, move to the left with increasing cluster size due to the variation in the ε values, to end up in the fcc(111) region for sufficiently large sizes. Looking at the crossover sizes predicted by this method, we find good agreement with those found within our atomistic calculations.

V. DISCUSSION AND CONCLUSIONS

In papers I and II, the low-energy structures of metal clusters adsorbed on MgO(001) have been investigated by a combination of computational methods. Simulation results have been compared also to those derived from the Wulff–Kaischew construction. Here we focus on summarizing the results for Pt and Pd, even though some comparison with Ag and Au will be made.

For all metals, the preferred structures of clusters at small sizes is in fcc(001) cube-on-cube epitaxy with the substrate. These fcc(001) clusters may either be in competition with fcc(111) clusters (in the case of Au and Pd) or with decahedral fragments (as in Ag and Pt). As size increases, metals behave differently.

In Ag, the fcc(001) clusters are favorable up to $N=3000$ at least. In Au the crossover is around $N=1200$, but both epitaxies are in close competition in the whole size range. As shown in Ref. 1, these results well agree with the available experimental observations.

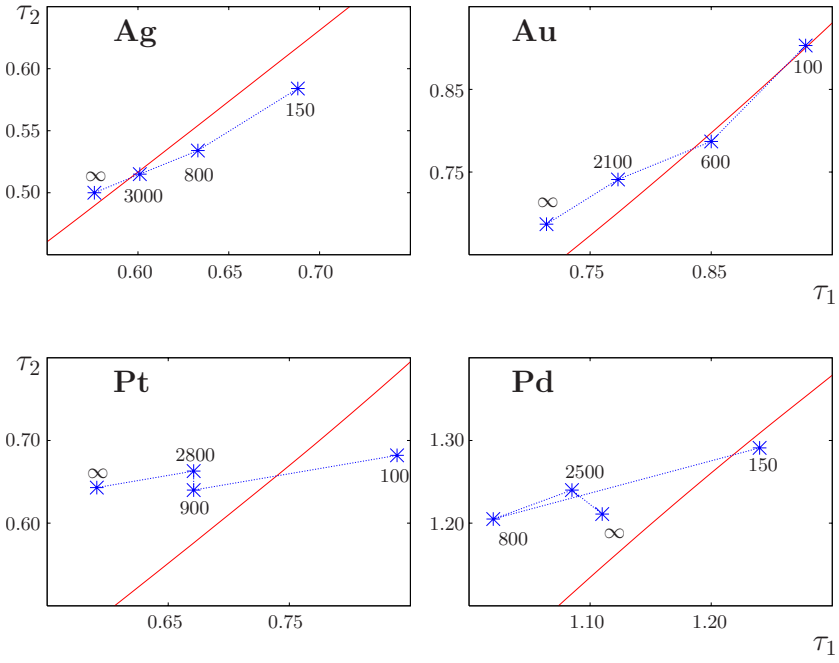

FIG. 7. (Color online) Same as in Fig. 5, but now four points correspond to each system, to take into account the variation in the adhesion energies with cluster size. For each point, we indicate the corresponding approximate cluster size. For $N\to\infty$ the points are in the upper left part of the (τ_1,τ_2) plane for all metals, corresponding to the (111) epitaxy, as follows from Fig. 5. With decreasing size, the points approach the dividing line of the plane and end in the lower right part, which corresponds to the (001) epitaxy. The irregular behavior of the Pt and Pd points is due to the appearance of dislocations. These appear at sizes which are far above the crossover size between epitaxies.

According to our calculations, Pt/MgO(001) clusters are fcc(001) at small sizes. For $N<200$, these are followed by decahedral clusters, while fcc(111) clusters are the highest in energy. A first crossover between decahedra and fcc(111) clusters is found around size 200, followed by a second crossover between (001) and (111) clusters at $N\simeq 550$. The latter becomes clearly the most favorable for large sizes. Such a rather sharp crossover is common to Pd, but not to Au. It can be interpreted by noting that Pt and Pd present a lattice mismatch, which induces a strong size dependence of the adhesion energy of (001) facets. When comparing with experiments,[22] the comparison is not completely straightforward. The fact that in clusters grown below 1000 K both epitaxies are observed is in qualitative agreement with our findings, which predict a competition between them. However, the experimentally observed transition to fcc(001) structures at high temperatures is not easily interpreted by our calculations. More studies are necessary.

The case of Pd/MgO(001) presents the most problematic comparison with the experiments for large sizes, while for sizes below 200 atoms the results agree well with experiments and DF calculations.[25,26] In fact, our calculations predict a crossover from (001) to (111) epitaxy around $N=200$. Some experimental data indeed indicate the presence (in some cases marginal) of fcc(111) clusters,[28–31] but at larger sizes.[28] Other experiments are in favor of the (001) epitaxy only,[27,32–34] up to the largest observed sizes (of several nanometers, thus containing many thousands of atoms).

This discrepancy between our results and the experiments may originate from different causes. Pd has a strong interaction with the substrate and the largest lattice mismatch. This causes a rather strong dependence of the adhesion energy on size in the (001) epitaxy (see Fig. 6). Compared to DF data, our metal-metal interactions underestimate surface energies, while the metal-substrate interaction is fitted on DF values. From the Wulff–Kaischew construction it follows that our simulated clusters are flatter than those that one would find from a full DF calculation, and probably flatter than those produced in experiments. Therefore, our simulated clusters adhere to the substrate with larger facets. This disfavors the (001) epitaxy, which worsens its adhesion per unit area as the contact area increases. In order to verify this effect we reparametrized the metal-metal part of the interaction potential in order to obtain higher surface energies that are in good agreement with the DF calculations. As can be seen in Fig. 8, there is a neat effect, which shows that crossover sizes are quite sensitive to changes in surface energies. In fact, the results of the new parametrization shift the transition size from 200 to about 750 atoms, thus going in the direction of a better agreement with the experimental data.

Furthermore, we note that it is not easy to disentangle thermodynamic, kinetic, support, etc. effects[8,35,36] and compare our low-energy structures with the outcome of experiments in a straightforward way. For example, a possible hypothesis to solve the discrepancy between experiment and theory is that in conditions of high flux and on surfaces rich in local defects (whose influence on the cluster structure can be expected to be minor in the limit of large sizes) the clusters nucleate on regular terraces or local defects and are thus free to realize a transition from (001) to (111) epitaxy, whereas when the clusters grow on extended defects such as steps (as those shown in Ref. 37) the influence of the support is sufficient to invert the energetic preference between (001) and (111) epitaxies. More studies are however necessary to support this hypothesis.

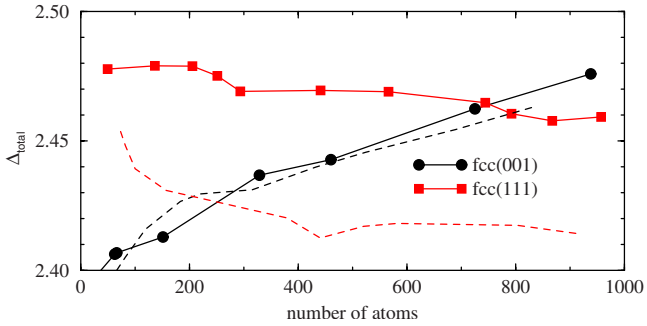

FIG. 8. (Color online) Comparison of the crossover between fcc(001) and fcc(111) epitaxies in Pd/MgO(001), according to different parametrization of the metal-metal interaction potential. Δ_{total} is given in eV. The results of the reparametrized Pd–Pd potential correspond to the full lines, which cross at about 750 atoms. Dashed lines reproduce the results of Fig. 4, with a crossover at about 200 atoms. The dashed lines have been shifted rigidly upwards by the same amount to achieve a more evident comparison with the full lines.

Finally we note that the transition between different epitaxies can be treated within the framework of the Wulff–Kaischew construction. This construction predicts that the asymptotic epitaxy for large cluster sizes should be (111), not only for Pd and Pt, but also for the metals, Ag and Au, treated in paper I. By incorporating into the Wulff–Kaischew framework size-dependent adhesion energies, we were able to reproduce the crossover toward the (001) epitaxy in the correct size range. This shows that the size dependence of the adhesion energy per unit contact area has a key role in driving the transition between epitaxies.

ACKNOWLEDGMENTS

We acknowledge financial support from the European Community Sixth Framework Program for the GSOMEN project (Project No. NMP4-CT-2004-001594), from the French National Agency for Research under the project SIMINOX (Project No. ANR-06-NANO-009-01), and from the Université Franco-Italienne under the program Galileo. G.R. acknowledges *L'Oréal Italia e UNESCO per le Donne e la Scienza*, 2007 edition, for a research fellowship. A.F. is grateful to Clemens Barth for interesting and useful discussions.

APPENDIX: WULFF-KAISCHEW CONSTRUCTION FOR (001) AND (111) EPITAXIES

Here we derive the formulas for the energy of fcc(001) and fcc(111) clusters by means of the Wulff-Kaischew construction.

1. In vacuum

In vacuum the clusters have the shape of truncated octahedra. An ideal octahedron is formed of two pyramids of height h with a square basis; from a truncated octahedron six little pyramids of height $q=xh$ are missing. x depends on

$$\sigma = \frac{\gamma_{(111)}}{\gamma_{(001)}}; \tag{A1}$$

by Wulff's theorem

$$x = 1 - \frac{1}{\sqrt{3}\sigma}. \tag{A2}$$

The inequalities

$$\frac{1}{\sqrt{3}} < \sigma < \frac{1}{\sqrt{3}-1} \tag{A3}$$

must hold; indeed for $\sigma \leq 1/\sqrt{3}$ the cluster would be an ideal octahedron, for $\sigma > 1/(\sqrt{3}-1)$ a cube, while in between these values the cluster is a truncated octahedron.

A truncated octahedron has 14 facets, 6 of type (001) and 8 of type (111). Letting $s_{(001)}$ and $s_{(111)}$ be their respective areas, we find

$$s_{(001)} = 2x^2h^2, \quad s_{(111)} = \frac{\sqrt{3}}{2}(1-3x^2)h^2. \tag{A4}$$

The volume is

$$V = V_0 = \tfrac{4}{3}(1-3x^3)h^3 \tag{A5}$$

and (using here and in the following $\gamma_{(001)}$ as the unit of energy/area) the total surface energy is

$$E_0 = 4\frac{1-3x^3}{1-x}h^2\gamma_{(001)} = \frac{[36(1-3x^3)]^{1/3}}{1-x}V^{2/3}\gamma_{(001)}. \tag{A6}$$

2. On the surface

On the surface, not only σ, but also τ_1 and τ_2,

$$\tau_1 = \frac{|\varepsilon_{(001)}|}{\gamma_{(001)}}, \quad \tau_2 = \frac{|\varepsilon_{(111)}|}{\gamma_{(111)}} \tag{A7}$$

are important parameters. When the cluster is adsorbed on the surface, a further cutting of its free vacuum shape takes place. For a given h, a part of the cluster is cut. The (negative) volume of this part is ΔV, which can be calculated by

$$\Delta V = -\int_0^p S(z)dz, \tag{A8}$$

where p is the height of the part which is cut and S is the area of the x-y cross section of the volume which is cut. S depends on z, with $0 \leq z \leq p$.

A remark is necessary here. In comparing the two epitaxies, clusters of the same size must be considered. In fact, the question that we wish to answer in the following is: Given surface and adhesion energies, what is the best epitaxy for a truncated octahedral cluster of a given size?

This means that the volume of the cluster after all cuts (at free and supported surfaces) must be the same for both epitaxies. Therefore, clusters corresponding to different values of h will be compared, because h will be determined in order to produce the same volume for both epitaxies.

In the subsequent formulae we suppose τ to be less than 1. The quantity τ is positive and its value can be both larger and smaller than one. When $\tau < 1$, less than half of the unsupported cluster is cut due to its contact with the substrate. There is, however, a duality property which allows us to suppose $\tau < 1$ and pass to the case of $2-\tau$ when required by $\tau > 1$ (this is the case of Pd).

Letting energy and volume to be

$$E = A(\tau)h^2\gamma_{(001)}, \quad V = B(\tau)h^3, \tag{A9}$$

the duality is expressed by

$$A(2-\tau) + A(\tau) = A(0), \quad B(2-\tau) + B(\tau) = B(0), \tag{A10}$$

where, as we have seen,

$$A(0) = 4\frac{1-3x^3}{1-x}, \quad B(0) = \frac{4}{3}(1-3x^3). \tag{A11}$$

We will compare explicitly two situations, evaluating the surface energy of two clusters of the same volume but with different facets adhering to the substrate, namely, type (001) (orientation 1) or type (111) (orientation 2).

a. fcc(001) epitaxy

When the cluster is supported on (001) (orientation 1) there are:

-One (001) facet at the cluster bottom (in contact with the substrate, of area $S_{(001)}$),
-One (001) facet on top of the cluster (of area $s_{(001)}$),
-Four lateral (001) facets (of area $s'_{(001)}$ each),
-Four lateral (111) facets in the lower half of the cluster (of area $s'_{(111)}$ each), and
-Four lateral (111) facets in the upper half of the cluster (of area $s_{(111)}$ each).

Therefore, the total cluster energy is given by

$$E_1 = 4(s_{(111)} + s'_{(111)})\gamma_{(111)} + (s_{(001)} + 4s'_{(001)})\gamma_{(001)} + S_{(001)}(\gamma_{(001)} - |\varepsilon_{(001)}|). \tag{A12}$$

Let $y = p/h = \tau_1(1-x)$. Here two cases must be distinguished:

First case: $\tau_1 < (1-2x/1-x)$. In this case, the four lateral (001) facets are not cut by the contact with the substrate. Then

$$s'_{(001)} = s_{(001)}, \tag{A13}$$

$$s'_{(111)} = \frac{\sqrt{3}}{2}(1-3x^2-2xy-y^2)h^2, \tag{A14}$$

$$S_{(001)} = 2(x+y)^2h^2, \tag{A15}$$

$$\Delta V = -\tfrac{2}{3}[(x+y)^3 - x^3]h^3. \tag{A16}$$

Second case: $(1-2x/1-x)<\tau_1<1$ In this case the four lateral (001) facets are cut

$$s'_{(001)}=[2x^2-(y+2x-1)^2]h^2<s_{(001)}, \tag{A17}$$

$$s'_{(111)}=\frac{\sqrt{3}}{2}(3-5x-y)(1-x-y)h^2, \tag{A18}$$

$$S_{(001)}=[2(x+y)^2-4(y+2x-1)^2]h^2, \tag{A19}$$

$$\Delta V=-\tfrac{2}{3}[(x+y)^3-x^3-2(y+2x-1)^3]h^3. \tag{A20}$$

In both cases the volume is obtained by subtracting $V=V_0-|\Delta V|$ (ΔV is negative), V is found as $V=V(h,x,y)$, which also means $V=V(h,\sigma,\tau_1)$. Inverting with respect to h, one finds $h=h(V,\sigma,\tau_1)$, from which the total interface energy of the (001) epitaxy $E_1=E_1(V,\sigma,\tau_1)$ follows.

b. fcc(111) epitaxy

When the cluster is supported on (111) (orientation 2) there are:

-One (111) facet at the cluster bottom (in contact with the substrate, of area $S_{(111)}$),
-One (111) facet on top of the cluster (of area $s_{(111)}$),
-Three lateral (001) facets in the lower half of the cluster (of area $s'_{(001)}$ each),
-Three lateral (001) facets in the upper half of the cluster (of area $s_{(001)}$ each),
-Three lateral (111) facets in contact with the facet at the cluster bottom (of area $s'_{(111)}$ each), and
-Three lateral (111) facets in contact with the facet at the cluster top (of area $s''_{(111)}$ each).

The energy is given by

$$E_2=(s_{(111)}+3s'_{(111)}+3s''_{(111)})\gamma_{(111)}+3(s_{(001)}+s'_{(001)})\gamma_{(001)}+S_{(111)}(\gamma_{(111)}-|\varepsilon_{(111)}|). \tag{A21}$$

Two cases must again be distinguished.

First case: $\tau_2<2x$. In this case, the three lateral (111) facets that are in contact with the cluster top are not cut. Then

$$s'_{(001)}=x(2x-\tau 2)h^2, \tag{A22}$$

$$s'_{(111)}=\frac{\sqrt{3}}{8}[(2-\tau_2)^2-4x^2-2(2x-\tau_2)^2]h^2, \tag{A23}$$

$$s''_{(111)}=s_{(111)} \tag{A24}$$

$$S_{(111)}=\frac{\sqrt{3}}{2}\left[\left(1+\frac{1}{2}\tau_2\right)^2-3x^2\right]h^2, \tag{A25}$$

$$\Delta V=-\tfrac{1}{24}\tau_2(12+6\tau_2+\tau_2^2-36x^2)h^3. \tag{A26}$$

Second case: $2x<\tau_2<1$. In this case, the three lateral (111) facets that are in contact with the cluster top are cut. Then

$$s'_{(001)}=0, \tag{A27}$$

$$s'_{(111)}=\frac{\sqrt{3}}{8}[(2-\tau_2)^2-4x^2]h^2, \tag{A28}$$

$$s''_{(111)}=\frac{\sqrt{3}}{8}(4-8x^2-\tau_2^2)h^2 \tag{A29}$$

$$S_{(111)}=\frac{\sqrt{3}}{4}[2+2\tau_2-\tau_2^2]h^2, \tag{A30}$$

$$\Delta V=-\left[\tfrac{1}{12}\tau_2(6+3\tau_2-\tau_2^2)-2x^3\right]h^3. \tag{A31}$$

In analogy with the case of E_1, $E_2=E_2(V,\sigma,\tau_2)$ can be calculated.

[1] R. Ferrando, G. Rossi, A. C. Levi, Z. Kuntová, F. Nita, G. Barcaro, A. Fortunelli, A. Jelea, C. Mottet, and J. Goniakowski, J. Chem. Phys. **130**, 174702 (2009).
[2] R. Ferrando, G. Rossi, F. Nita, G. Barcaro, and A. Fortunelli, ACS Nano **2**, 1849 (2008).
[3] W. Tian, H. P. Sun, X. Q. Pan, J. H. Yu, M. Yeadon, C. B. Boothroyd, Y. P. Feng, R. A. Lukaszew, and R. Clarke, Appl. Phys. Lett. **86**, 131915 (2005).
[4] C. R. Henry, Prog. Surf. Sci. **80**, 92 (2005).
[5] B. Mutaftschiev, *The Atomistic Nature of Crystal Growth* (Springer-Verlag, Berlin, 2001).
[6] C. Mottet and J. Goniakowski, J. Comput. Theor. Nanosci. **4**, 326 (2007).
[7] F. Baletto, R. Ferrando, A. Fortunelli, F. Montalenti, and C. Mottet, J. Chem. Phys. **116**, 3856 (2002).
[8] F. Baletto and R. Ferrando, Rev. Mod. Phys. **77**, 371 (2005).
[9] W. Vervisch, C. Mottet, and J. Goniakowski, Phys. Rev. B **65**, 245411 (2002).
[10] W. Vervisch, C. Mottet, and J. Goniakowski, Eur. Phys. J. D **24**, 311 (2003).
[11] J. F. M. Cillessen, R. M. Wolf, and D. M. de Leeuw, Thin Solid Films **226**, 53 (1993).
[12] J. Narayan, P. Tiwari, K. Jagannadham, and O. W. Holland, Appl. Phys. Lett. **64**, 2093 (1994).
[13] Y. Takai and M. Sato, Supercond. Sci. Technol. **12**, 486 (1999).
[14] M. Morcrette, A. Guitierrez-Llorente, W. Seiler, A. Laurent, and P. Barboux, J. Appl. Phys. **88**, 5100 (2000).
[15] R. Farrow, D. Weller, R. Marks, M. Toney, A. Cebollada, and G. Harp, J. Appl. Phys. **79**, 5967 (1996).
[16] P. McIntyre, C. Maggiore, and M. Natasi, Acta Mater. **45**, 869 (1997).
[17] P. McIntyre, C. Maggiore, and M. Natasi, Acta Mater. **45**, 879 (1997).
[18] B. M. Lairson, M. R. Visokay, R. Sinclair, S. Hagstrom, and B. M. Clemens, Appl. Phys. Lett. **61**, 1390 (1992).
[19] J. L. Menéndez, P. Caro, and A. Cebollada, J. Cryst. Growth **192**, 164 (1998).
[20] P. Andreazza, C. Andreazza-Vignolle, J. Rozenbaum, A.-L. Thomann, and P. Brault, Surf. Coat. Technol. **151–152**, 122 (2002).
[21] C. Gatel, P. Baules, and E. Snoeck, J. Cryst. Growth **252**, 424 (2003).
[22] J. Olander, R. Lazzari, J. Jupille, B. Mangili, J. Goniakowski, and G. Renaud, Phys. Rev. B **76**, 075409 (2007).
[23] J. Chen, M. Hupalo, M. Ji, C. Z. Wang, K. M. Ho, and M. C. Tringides, Phys. Rev. B **77**, 233302 (2008).
[24] F. Baletto, C. Mottet, and R. Ferrando, Phys. Rev. Lett. **84**, 5544 (2000).
[25] G. Rossi, C. Mottet, F. Nita, and R. Ferrando, J. Phys. Chem. B **110**, 7436 (2006).
[26] G. Barcaro, A. Fortunelli, F. Nita, G. Rossi, and R. Ferrando, Phys. Rev. Lett. **98**, 156101 (2007).
[27] C. R. Henry, Surf. Sci. Rep. **31**, 231 (1998).
[28] P. Nolte, A. Stierle, N. Kasper, N. Y. Jin-Phillipp, H. Reichert, A. Rühm, J. Okasinski, H. Dosch, and S. Schöder, Phys. Rev. B **77**, 115444 (2008).
[29] H. Fornander, J. Birch, L. Hultman, L. G. Petersson, and J. E. Sundgren, Appl. Phys. Lett. **68**, 2636 (1996).
[30] H. Fornander, L. Hultman, J. Birch, and J. E. Sundgren, J. Cryst. Growth **186**, 189 (1998).

[31] C. Revenant, F. Leroy, R. Lazzari, G. Renaud, and C. R. Henry, Phys. Rev. B **69**, 035411 (2004).
[32] G. Renaud and A. Barbier, Surf. Sci. **433–435**, 142 (1999).
[33] G. Renaud, A. Barbier, and O. Robach, Phys. Rev. B **60**, 5872 (1999).
[34] G. Renaud, R. Lazzari, C. Revenant, A. Barbier, M. Noblet, O. Ulrich, F. Leroy, J. Jupille, Y. Borensztein, C. R. Henry, J.-P. Deville, F. Scheurer, J. Mane-Mane, and O. Fruchart, Science **300**, 1416 (2003).
[35] G. Barcaro, E. Aprà, and A. Fortunelli, Chem. Eur. J. **13**, 6408 (2007).
[36] J. Oviedo, J. Fernandez-Sanz, N. Lopez, and F. Illas, J. Phys. Chem. B **104**, 4342 (2000).
[37] O. H. Pakarinen, C. Barth, A. S. Foster, and C. R. Henry, J. Appl. Phys. **103**, 054313 (2008).